nature neuroscience

Designer receptors show role for ventral pallidum input to ventral tegmental area in cocaine seeking

Stephen V Mahler[1], Elena M Vazey[1], Jacob T Beckley[1], Colby R Keistler[1], Ellen M McGlinchey[1], Jennifer Kaufling[1], Steven P Wilson[2], Karl Deisseroth[3], John J Woodward[1] & Gary Aston-Jones[1]

The ventral pallidum is centrally positioned within mesocorticolimbic reward circuits, and its dense projection to the ventral tegmental area (VTA) regulates neuronal activity there. However, the ventral pallidum is a heterogeneous structure, and how this complexity affects its role within wider reward circuits is unclear. We found that projections to VTA from the rostral ventral pallidum (RVP), but not the caudal ventral pallidum (CVP), were robustly Fos activated during cue-induced reinstatement of cocaine seeking—a rat model of relapse in addiction. Moreover, designer receptor–mediated transient inactivation of RVP neurons, their terminals in VTA or functional connectivity between RVP and VTA dopamine neurons blocked the ability of drug-associated cues (but not a cocaine prime) to reinstate cocaine seeking. In contrast, CVP neuronal inhibition blocked cocaine-primed, but not cue-induced, reinstatement. This double dissociation in ventral pallidum subregional roles in drug seeking is likely to be important for understanding the mesocorticolimbic circuits underlying reward seeking and addiction.

The ventral pallidum is a crucial node in the ventral striatopallidal circuits underlying reward-related behaviors, with major reciprocal connections to the accumbens, extended amygdala, limbic thalamus, substantia nigra (SN) and VTA[1–4]. Ventral pallidum neurons respond to rewards and their cues in animals and humans and are necessary for reward-seeking behaviors, leading to hypotheses that the ventral pallidum helps translate motivational states into appetitive behaviors[5–7].

However, the ventral pallidum is a heterogeneous structure, exhibiting medial-lateral and rostral-caudal variation in histological markers and connectivity patterns[1,4,8]. Notably, the ventromedial ventral pallidum (most of which is located subcommissurally, rostral of bregma in rat: RVP) receives dense afferents from the nucleus accumbens shell and projects strongly to the mediodorsal thalamus and VTA. The dorsolateral ventral pallidum (most of which is located sublenticularlly, caudal of bregma: CVP) instead receives afferents from the accumbens core and projects to SN and the subthalamic nucleus, in addition to VTA[1,9]. This topography implies the involvement of ventral pallidum subregions in functionally distinct mesolimbic circuits.

Functional heterogeneity between ventral pallidum subregions has also been reported. *In vitro*, RVP and CVP neurons differ in several ways: many RVP neurons have spiny dendrites, glutamatergic afferents, hyperpolarized membrane potentials and no spontaneous action potentials[10]. Interestingly, these characteristics are more typical of accumbens medium spiny neurons than 'classical' ventral pallidum neurons. In contrast, CVP neurons have more classically pallidal characteristics, including aspiny dendrites, GABAergic inputs, depolarized membrane potentials and spontaneous action potentials. Notably, neuronal firing during rat cocaine self-administration varies depending on mediolateral and rostrocaudal localization within the ventral pallidum[11], and ventral pallidum rostrocaudal variation exists in neuronal cytoarchitecture, *in vivo* firing rates, sensitivity to the rewarding effects of electrical stimulation and microinjected drugs, opioid agonist–induced hedonic responses to tastes and functional magnetic resonance imaging (fMRI) activation to emotionally arousing pictures[12–19].

However, little is known about how such heterogeneity contributes to the functions of the ventral pallidum within wider mesolimbic circuits. In rats, CVP provides tonically active GABA inputs to VTA and SN that gate the firing of subpopulations of dopamine neurons and modulate reward seeking[20]. However, ventral pallidum neurons are also acutely activated by reward-associated cues[6,21,22], and ventral pallidum projections to VTA are activated during cue-induced reinstatement of cocaine seeking[23]. How does functional-anatomical heterogeneity affect the regulation of VTA by the ventral pallidum and the role of this circuit in drug seeking?

We sought to examine the roles of ventral pallidum subregions and their VTA projections in relapse to cocaine seeking. We examined Fos activation of RVP and CVP projections to VTA and inactivated these subregions or their projections to midbrain dopaminergic regions during reinstatement of cocaine seeking using designer receptors exclusively activated by designer drugs (DREADDs)[24]. DREADDs utilize endogenous G-protein signaling pathways but do not affect neuronal activity in the absence of their otherwise inert, exogenously administered ligand, clozapine-N-oxide (CNO). The G_i-coupled (hM4Di) DREADDs used here thereby allow transient inactivation of defined neuronal populations[25]. We also show that they can be used to manipulate axonal terminals of DREADD-expressing neurons

[1]Department of Neurosciences, Medical University of South Carolina, Charleston, South Carolina, USA. [2]Department of Pharmacology, Physiology and Neuroscience, School of Medicine, University of South Carolina, Columbia, South Carolina, USA. [3]Department of Bioengineering and Psychiatry and Behavioral Sciences, Stanford University, Stanford, California, USA. Correspondence should be addressed to S.V.M. (mahler@musc.edu).

Received 12 December 2013; accepted 28 January 2014; published online 2 March 2014; doi:10.1038/nn.3664

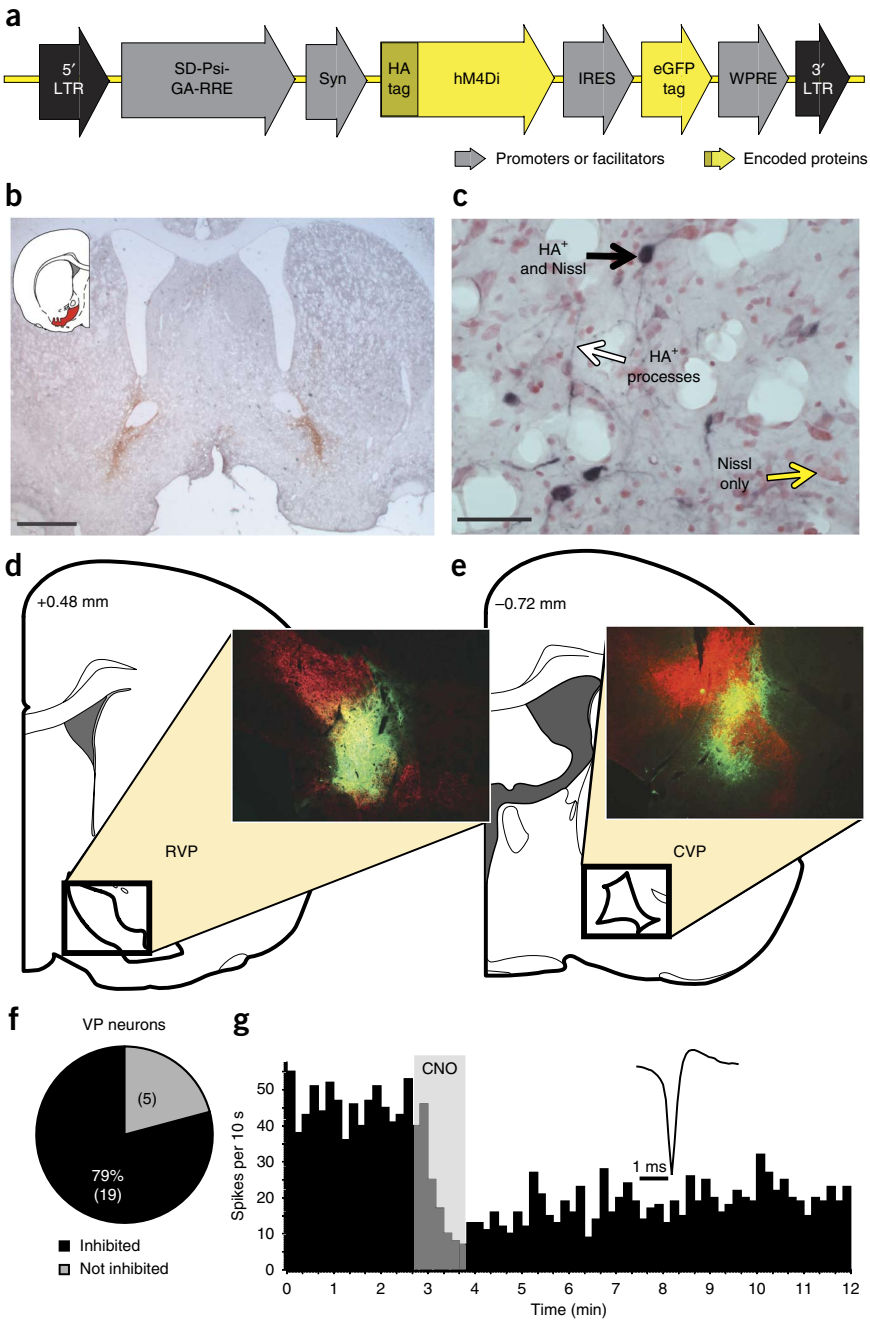

Figure 1 hM4Di inhibitory DREADD expression and function. (**a**) The *Syn-hM4Di-HA-GFP* lentivirus used to express hM4Di DREADDs under a neuronal-specific human synapsin promoter (*Syn*) in RVP or CVP. LTR, long terminal repeat; IRES, internal ribosome entry site; eGFP, enhanced GFP; WPRE, WHV post-transcriptional regulatory element; SD, splice donor site; Psi, encapsidation signal; GA, truncated GAG sequence; RRE, Rev response element. (**b**) Typical staining for HA-tagged hM4Di after bilateral injections into RVP. Scale bar, 1 mm. (**c**) HA-tagged hM4Di receptors are expressed on cell bodies and processes (black staining) in the ventral pallidum (neutral red counterstain). Scale bar, 50 μm. (**d**) Typical HA expression (green) in RVP contained largely within the ventral pallidum borders (defined with substance P counterstain in red). (**e**) Typical HA expression in CVP contained largely within the ventral pallidum borders (as defined in **d**). Images in **b**–**e** are representative of DREADD expression seen in the experimental groups (with *n* numbers listed in the main text). The width of the images in **d** and **e** is 2.65 mm. (**f**) Inhibition of firing rates in neurons ($n = 24$ total) from animals with *Syn-hM4Di-HA-GFP* expression in RVP or CVP and local application of 100 μM CNO onto extracellularly recorded ventral pallidum (VP) neurons *in vivo* (with a double-barrel glass pipette). (**g**) Typical change in discharge rate of a ventral pallidum neuron (waveform inset) after local CNO application (shaded region).

to inactivate particular monosynaptic pathways (for example, RVP-VTA) or to disrupt functional connectivity between specific neuronal populations (for example, RVP and VTA dopamine neurons). We demonstrate a double dissociation between the rostral and caudal ventral pallidum in cued as compared to cocaine-primed reinstatement, respectively, and show that cued cocaine seeking is dependent on RVP projections to VTA and complex interactions with dopaminergic and nondopaminergic neurons there.

RESULTS

Validation of ventral pallidum DREADDs

We used a DREADD-based strategy to remotely control ventral pallidum neurons *in vivo* and manipulate the ventral pallidum–VTA circuit. We injected a synapsin-driven lentiviral vector yielding expression of the G_i-coupled DREADD, hM4Di[24], or a control virus lacking the DREADD gene (*Syn-GFP*) into RVP or CVP and allowed animals to survive for at least 6 weeks before analyzing the brain tissue for virus expression. The *Syn-hM4Di-HA-GFP* virus (**Fig. 1a**) caused robust hM4Di expression within RVP or CVP (visualized with immunoreactivity for the hemagglutinin (HA) tag or a GFP reporter). These injections yielded limited expression outside the borders of the ventral pallidum (<30% labeling outside the ventral pallidum borders; **Figs. 1** and **2d** and **Supplementary Fig. 1**). The *Syn-hM4Di-HA-GFP* and *Syn-GFP* viruses yielded comparable zones of somatic GFP or hM4Di expression centered at the injection site (GFP: 0.82 (0.21) mm^3 (mean (s.e.m.)); hM4Di: 0.89 (0.05) mm^3).

We then used *in vivo* electrophysiology to functionally validate hM4Di receptor expression. In isofluorane-anesthetized rats, local CNO microinjection (60 nl, 100 μM) inhibited ventral pallidum neurons ($n = 24$ cells, 60.3 ± 6.6% (mean ± s.e.m., normalized to the pre-CNO firing rate for each cell) decrease in firing, $Z = -2.54$, $P = 0.011$; **Fig. 1f**,**g**). Local microinjection of CNO similarly affected RVP neurons (11/13 cells inhibited) and CVP neurons (8/11 inhibited), with 58.2 ± 8.7% and 63.2 ± 10.6% inhibition, respectively. Pre-CNO firing rates in RVP (6.4 ± 2.0 Hz) were lower than in CVP (24.8 ± 5.3 Hz, $P = 0.007$, $t_{12} = 3.26$), as reported previously[10,12].

Double dissociation of ventral pallidal roles in reinstatement

Next we examined whether transient DREADD-mediated inhibition of RVP or CVP would attenuate either cued or cocaine-primed (10 mg per kg body weight) reinstatement of cocaine seeking after

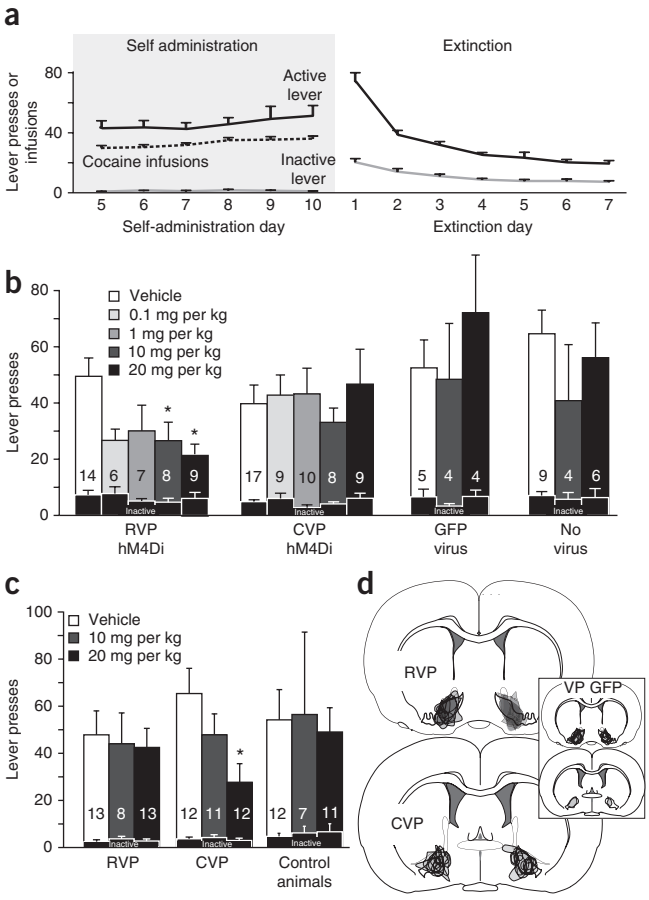

Figure 2 Effects of inactivating the rostral or caudal ventral pallidum on reinstatement of cocaine seeking. (**a**) Daily cocaine infusions and active or inactive lever presses (mean ± s.e.m.) for the last 6 days of criterion self administration (>10 infusions per day) and active or inactive lever presses for the first 7 days of extinction training. (**b**) Active lever presses during cue-induced reinstatement after different doses of the DREADD agonist CNO (the various doses are distinguished by bar shading: vehicle or 0.1, 1, 10 or 20 mg per kg body weight) in animals with bilateral RVP or CVP *Syn-hM4Di-HA-GFP* virus expression, bilateral ventral pallidum control virus (*Syn-GFP*) expression or no virus expression. Inactive lever presses during reinstatement are shown with overlaid black bars. $^*P = 0.001$ for vehicle compared to 10 mg per kg body weight CNO; $^*P = 0.015$ for vehicle compared to 20 mg per kg body weight CNO (analysis of variance (ANOVA) with Bonferroni correction *post hoc*). (**c**) Active and inactive lever presses during cocaine-primed reinstatement after vehicle or different doses of CNO (10 or 20 mg per kg body weight) in animals with RVP or CVP *Syn-hM4Di-HA-GFP* virus expression or control animals (*Syn-GFP* or no virus expression). $^*P = 0.008$ for vehicle compared to 20 mg per kg body weight CNO (ANOVA with Bonferroni correction *post hoc*). The data in **b** and **c** are shown as the mean ± s.e.m. (**d**) The anatomical localization of virus expression sites (as visualized with HA or GFP immunoreactivity) represented for animals injected with *Syn-hM4Di-HA-GFP* in RVP (black areas) or CVP (gray areas) or with *Syn-GFP* (gray areas; inset).

cocaine self-administration and extinction (**Fig. 2a**). CNO (0, 0.1, 1, 10 or 20 mg per kg body weight) attenuated cued reinstatement in rats with hM4Di expression in RVP but not in animals with comparable DREADD expression in CVP (RVP: $n = 16$ rats, $F_{4,39} = 4.0$, $P = 0.008$; CVP: $n = 17$ rats, $F_{4,46} = 0.59$, $P = 0.68$; **Fig. 2b**). In contrast, CNO (0, 10 or 20 mg per kg body weight) injections attenuated cocaine-primed reinstatement only in animals with hM4Di expression in CVP but not in RVP (RVP: $F_{2,29} = 0.45$, $P = 0.64$; CVP: $F_{2,31} = 3.48$, $P = 0.04$; **Fig. 2c**), revealing a double dissociation between RVP and CVP for reinstatement elicited by cues as compared to cocaine.

The zones in which hM4Di inhibition was most effective at reducing cued reinstatement were centered in RVP, whereas effective sites for cocaine-primed reinstatement were centered in CVP (cue, ventral pallidum site × drug interaction: $F_{1,16} = 7.35$, $P = 0.015$; prime, ventral pallidum site × drug interaction: $F_{1,25} = 4.85$, $P = 0.037$). Inhibition of the ventral pallidum was sufficient for these effects, as cases with minimal (<5%) hM4Di expression outside the ventral pallidum borders showed equivalent reinstatement effects as those with more (<30%) encroachment of expression into adjacent areas (**Supplementary Fig. 1**). CNO had no effect in animals with either GFP virus injections (*Syn-GFP*, lacking the hM4Di gene; $n = 5$ rats; cue: $F_{2,11} = 0.58$, $P = 0.58$; prime: $F_{1,8} = 0.05$, $P = 0.83$) or no virus expression ($n = 9$ rats; cue: $F_{2,18} = 0.87$, $P = 0.44$; prime: $F_{2,24} = 0.28$, $P = 0.76$; control groups combined, cue: $F_{2,28} = 0.77$, $P = 0.47$; prime: $F_{2,31} = 0.22$, $P = 0.80$; **Fig. 2b**,**c**).

Fos activation of RVP-VTA projections during reinstatement

We next asked whether the role of RVP in cued reinstatement behavior involves projections to VTA. First we examined Fos expression in RVP or CVP VTA-projecting neurons during cued

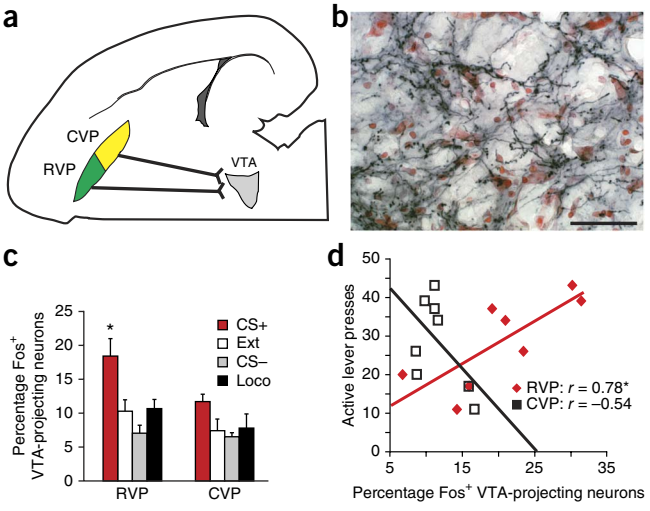

Figure 3 Rostral ventral pallidum projections to VTA are Fos activated during cued reinstatement. (**a**) Predominantly ipsilateral projections from RVP and CVP to VTA diagrammed in the horizontal plane. (**b**) Axon terminals in VTA express the anterogradely transported, HA-tagged hM4Di receptor (black axonal processes) after *Syn-hM4Di-HA-GFP* injection in ipsilateral RVP (red Nissl counterstain in VTA). Coronal view, scale bar, 50 µm. The image is representative of ventral pallidum axonal DREADD expression in VTA of the experimental animals (with *n* numbers listed in the main text). (**c**) Percentages (mean ± s.e.m.) of VTA-projecting (CTb^+) RVP or CVP cells that express Fos after cue-induced reinstatement (CS+) or control behavioral conditions in which animals were exposed to the extinguished self-administration environment without cues or cocaine (Ext), a tone or light stimulus not associated with cocaine (CS–) or a locomotion-enhancing novel environment (Loco). A greater proportion of VTA-projecting neurons in RVP were Fos activated in CS+ than in control animals ($^*P = 0.01$ for CS+ compared to Ext; $^*P = 0.005$ for CS+ compared to CS–; $^*P = 0.025$ for CS+ compared to Loco; one-way ANOVA with *post hoc* Tukey HSD). No significant behavior-specific activation of VTA-projecting neurons was detected in CVP. The data are shown as the mean ± s.e.m. (**d**) Correlation of cue-induced reinstatement behavior with Fos activation of VTA-projecting neurons in RVP ($^*P = 0.02$, Pearson correlation) and CVP ($P = 0.16$, nonsignificant Pearson correlation).

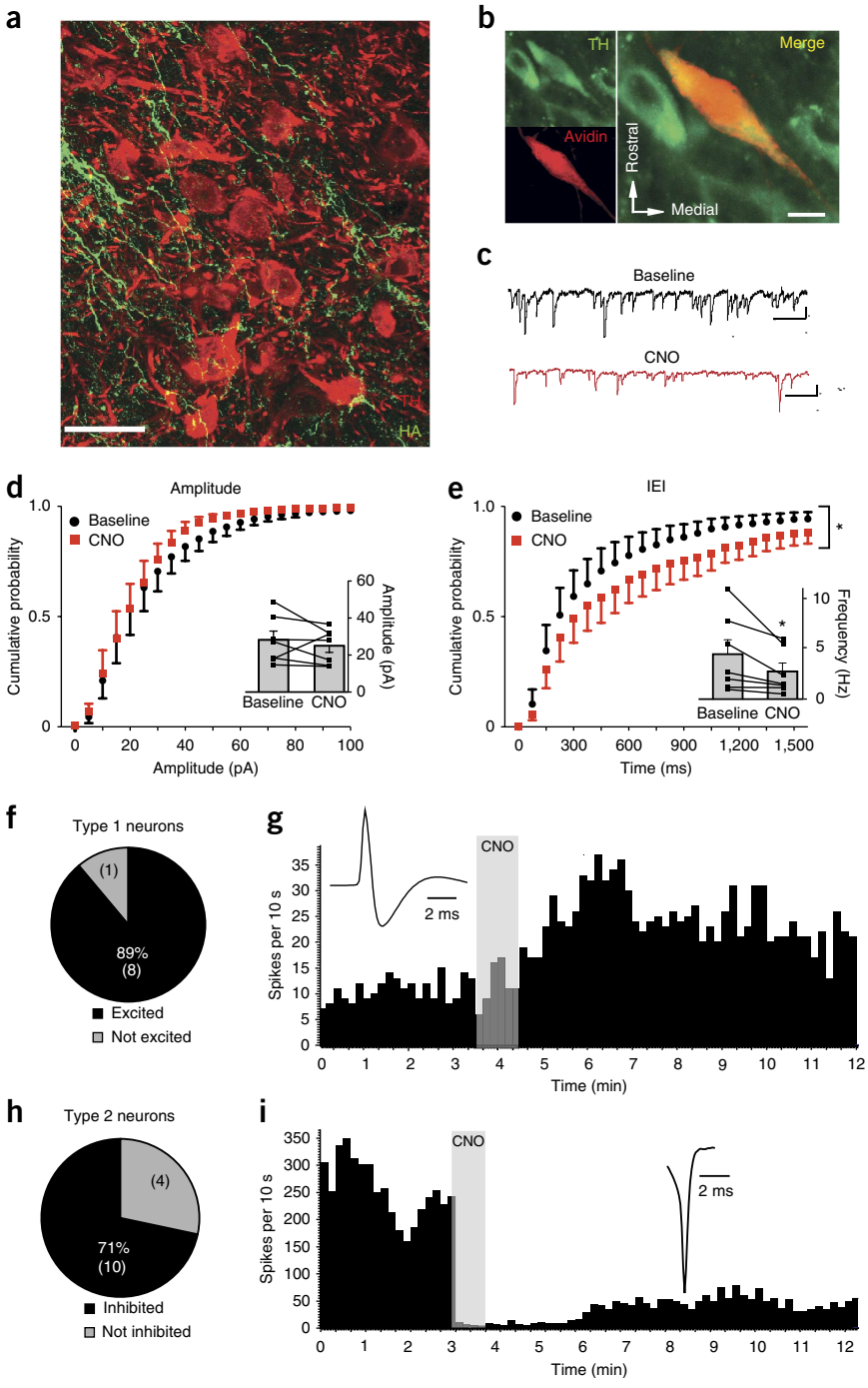

Figure 4 Inactivating rostral ventral pallidum afferents modulates VTA cell firing. (**a**) hM4Di receptors (green) are expressed on RVP axon terminals in the vicinity of TH-labeled dopamine neurons (red) in VTA. Scale bar, 30 µm. The image is representative of ventral pallidum axonal DREADD expression in VTA of experimental animals (with *n* numbers listed in the Online Methods). (**b**) Slice electrophysiology experiments in which recorded neurons were filled with biotin, labeled with avidin (red) and identified as dopaminergic by colabeling for TH (green). Scale bar, 10 µm. (**c**) Representative traces from VTA dopamine neurons in baseline conditions (top, black) and after CNO (bottom, red; vertical scales, 20 pA; horizontal scales, 200 ms). (**d**) The effect of CNO on the cumulative distribution or mean (inset) sIPSC amplitude. In the larger graph, the data are represented as the mean ± s.e.m.; the lines in the inset connect raw values for individual cells, and the bars show the mean ± s.e.m. (**e**) The shift in IEI cumulative distribution (*$P = 0.0002$ for baseline compared to CNO; two-way ANOVA) and mean sIPSC frequency (*$P = 0.046$ for baseline compared to CNO (inset); *t* test) after CNO. The data in the larger graph are shown as the mean ± s.e.m.; the lines in the inset connect raw values for individual cells, and the bars show the mean ± s.e.m. (**f**) *In vivo* excitation of putatively dopaminergic type 1 neurons ($n = 9$ total) in VTA by local application of CNO in the vicinity of hM4Di-expressing RVP terminals in VTA. (**g**) Rate histogram demonstrating the effect of local CNO application *in vivo* (60 nl; shaded region) on the firing of a type 1 neuron (waveform inset) in VTA of a RVP-hM4Di animal. (**h**) Inhibition of fast-firing, short-waveform type 2 neurons ($n = 14$ total) by local application of CNO *in vivo* in the vicinity of hM4Di-expressing RVP terminals in VTA. (**i**) Example change in the discharge rate of a type 2 neuron (waveform inset) in VTA after local CNO application *in vivo* (60 nl; shaded region) in a RVP-hM4Di animal.

reinstatement or control behaviors (**Fig. 3a** and **Supplementary Fig. 2**). We injected the retrograde tracer cholera toxin β subunit (CTb) into the rostral or caudal VTA. We trained animals ($n = 25$) to intravenously self-administer cocaine plus concurrently presented cues, extinguished this behavior and then gave them a 2-h cue-induced reinstatement test or control behavioral test (Online Methods). We euthanized the animals immediately after this test session and co-stained ventral pallidum slices for Fos and CTb.

In RVP, VTA-projecting (CTb^+) neurons were Fos activated during cued cocaine seeking ($n = 8$ rats) but not during exposure to the extinguished self-administration chamber ($n = 7$), a novel environment ($n = 6$) or a familiar, non–cocaine associated stimulus ($n = 4$; $F_{3,21} = 6.6$, $P = 0.002$; **Fig. 3c**). Unlike RVP, CVP projections to VTA were not significantly activated during cued reinstatement ($F_{3,21} = 2.3$, $P = 0.11$; **Fig. 3c** and **Supplementary Fig. 2**). Moreover, in individual cued cocaine-seeking animals, the degree of Fos activation of VTA afferents from RVP, but not CVP, was positively correlated with the degree of cue-induced cocaine-seeking behavior (RVP: $r = 0.78$, $P = 0.02$; CVP: $r = -0.54$, $P = 0.16$; **Fig. 3d** and **Supplementary Fig. 2d**), indicating that more activity in RVP efferents to VTA is associated with more cue-triggered drug seeking.

Validating inhibition of RVP-VTA projection with DREADDs

The hM4Di DREADD is trafficked axonally, as evidenced by numerous HA^+ fibers and terminals that are reliably observed in the ventral midbrain after injection of hM4Di vector in RVP or CVP (**Figs. 3b** and **4a** and **Supplementary Fig. 3d,e**). We examined whether modulation of G_i-coupled signaling in ventral pallidum axon terminals in VTA by local CNO application would alter the activity of VTA neurons. First we recorded spontaneous inhibitory postsynaptic currents (sIPSCs) from dopamine neurons (verified by tyrosine hydroxylase (TH) immunoreactivity) in VTA slices from rats that

were injected at least 6 weeks previously with the hM4Di vector in RVP ($n = 7$ rats; **Fig. 4b**,**c**). Perfusion with 5 μM CNO had no effect on sIPSC amplitude ($t_6 = 0.94$, $P = 0.38$; **Fig. 4d**) but decreased the frequency ($t_6 = 2.50$, $P = 0.046$) and shifted the cumulative distribution of interevent intervals (IEIs) to the right (main effect of IEI duration: $F_{21,264} = 22.18$, $P = 0.0001$; CNO treatment: $F_{1,264} = 14.42$, $P = 0.0002$; **Fig. 4e**). In slices from *Syn-GFP*–injected animals ($n = 5$ cells), which also expressed GFP in RVP neurons and VTA axons, CNO had no effect on sIPSC amplitude ($t_4 = 0.47$, $P = 0.67$) or IEIs ($t_4 = 0.39$, $P = 0.80$; **Supplementary Fig. 4**). These findings indicate that activation of hM4Di DREADDs on ventral pallidum terminals in VTA decreased GABA release onto VTA dopamine neurons.

We confirmed this finding *in vivo*, demonstrating that intra-VTA microinjection of CNO in rats previously injected with *Syn-hM4Di-HA-GFP* in RVP (RVP-hM4Di rats) significantly increased the firing rate (82.5 ± 50.2% increase) in 8 of 9 type 1 neurons (those meeting conventional electrophysiological criteria for VTA dopamine neurons[26]; $P = 0.03$; $t_7 = 2.63$; **Fig. 4f**,**g**). Conversely, 10 of 14 fast-spiking, short-waveform type 2 VTA neurons (not conventionally dopamine-like) were inhibited (−60.5 ± 12.0% change in discharge) after intra-VTA microinjection of CNO in RVP-hM4Di rats ($P = 0.003$; $t_9 = 3.93$; **Fig. 4h**,**i**).

Inhibiting RVP terminals in VTA blocks cued reinstatement

Next we examined effects of inactivating ventral pallidum terminals in VTA on cued or cocaine-primed reinstatement behavior. We microinjected (in a counterbalanced order on separate days) RVP-hM4Di animals ($n = 28$) with CNO (1 mM, 0.3 μl per side) or vehicle (artificial cerebrospinal fluid (aCSF)) into VTA ($n = 17$ rats) or SN ($n = 11$) 5 min before cued or primed reinstatement (two tests each per animal; **Fig. 5a**). We also injected CVP-hM4Di animals ($n = 9$) with CNO (0 or 1 mM, 0.3 μl) into VTA and then tested them on cued or primed reinstatement (**Fig. 5a** and cannulae sites in **Supplementary Fig. 5**). Inhibition of RVP terminals in VTA with local CNO selectively attenuated cued but not primed reinstatement (cue: $F_{1,16} = 27.87$, $P = 0.000075$; prime: $F_{1,16} = 0.01$, $P = 0.92$; **Fig. 5b**), indicating that activation of the RVP projection to VTA is required for drug cues to drive reinstatement of cocaine seeking. In contrast, inactivating RVP terminals in SN or CVP terminals in VTA had no effects on cued or primed reinstatement (RVP-SN inhibition, cue: $F_{1,10} = 0.21$, $P = 0.66$; prime: $F_{1,10} = 0.01$, $P = 0.92$; CVP-VTA inhibition, cue: $F_{1,8} = 0.84$, $P = 0.39$, prime: $F_{1,8} = 0.37$, $P = 0.56$; **Fig. 5d**,**f**). This result indicates that although CVP is necessary for cocaine-primed reinstatement (**Fig. 2c**), its VTA targets are not essential for this action.

Inactivating RVP projections to VTA in the absence of cues or priming injections failed to affect drug seeking after extinction ($n = 4$ rats; vehicle active lever presses: 8.7 ± 6.7 (mean ± s.e.m.); CNO: 4.3 ± 1.7; $F_{1,3} = 3.9$, $P = 0.14$). In RVP-hM4Di ($n = 11$) or CVP-hM4Di ($n = 6$) animals, neither intra-VTA ($n = 17$) nor intra-SN ($n = 6$) CNO had a significant effect on general locomotor behavior in a familiar environment (no main effect of drug or drug × time interactions; $F_s < 1.7$, $P_s > 0.11$; **Fig. 5c**,**e**,**g**), indicating that reinstatement effects of RVP-VTA inhibition are more likely motivational than motoric in nature.

RVP interacts with VTA dopamine neurons in reinstatement

VTA is a complex structure, with dopamine, GABA and glutamate projection neurons, as well as interneurons and other local connectivity[27–31]. Because ventral pallidum projections modulate dopamine and nondopamine neuron firing in VTA[32] (**Fig. 4**), we asked whether reinstatement behavior is affected by contrahemispheric disconnection of RVP from VTA dopamine neurons. In transgenic rats that express Cre recombinase in TH neurons (TH::Cre$^+$ rats)[33], we unilaterally transduced RVP neurons with the *Syn-hM4Di-HA-GFP* lentivirus described above. We also injected a double-floxed hM4Di adeno-associated virus (AAV) (*DIO-Syn-hM4Di-mCherry*; **Fig. 6a**) into the contralateral VTA ($n = 9$ rats) or SN ($n = 8$), yielding reliable and anatomically restricted hM4Di expression in unilateral dopamine neurons (**Fig. 6b**,**c** and **Supplementary Fig. 6**). A systemic CNO injection in these animals therefore functionally disconnected RVP inputs from midbrain dopamine cells bilaterally while sparing RVP connectivity with nondopaminergic VTA neurons (**Fig. 6d**). Control groups consisted of Cre$^+$ animals with unilateral VTA *DIO-Syn-hM4Di-mCherry* injections but no virus in RVP ($n = 6$ rats) or Cre$^-$ littermates ($n = 10$) with unilateral RVP hM4Di and contralateral VTA injections of *DIO-Syn-hM4Di-mCherry* (but no VTA hM4Di expression).

As shown in **Figure 6**, cue-induced reinstatement was markedly attenuated by disrupting the RVP-VTA dopamine circuit in this manner ($F_{1,8} = 37.97$, $P = 0.0003$; **Fig. 6e**). We found no effects after similarly disconnecting RVP from SN dopamine neurons ($F_{1,7} = 0.29$, $P = 0.61$) or after unilaterally inactivating either RVP ($F_{1,9} = 0.06$, $P = 0.81$) or VTA dopamine neurons ($F_{1,5} = 0.57$, $P = 0.48$) (**Fig. 6e**). This result indicates that intact connectivity between RVP (not CVP)

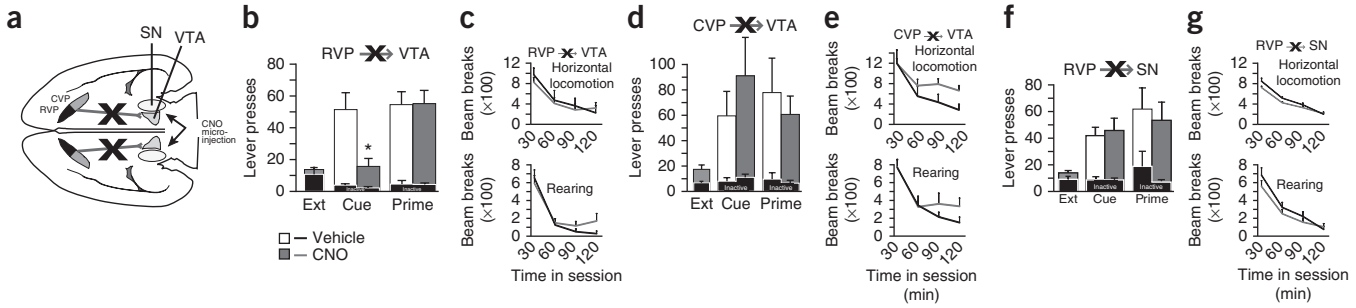

Figure 5 Inactivating rostral ventral pallidum projection to VTA blocks cued reinstatement. (**a**) Projections from RVP to VTA or SN or from CVP to VTA were transiently inactivated by local midbrain microinjection of CNO among ventral pallidum axon terminals expressing hM4Di receptors. (**b**) The effect of inactivation of VTA terminals from RVP on cue-induced (Cue) and cocaine-primed (Prime) reinstatement of cocaine seeking ($n = 17$). Also shown are active lever pressing during the last day of extinction training (Ext, bars at left) and reinstatement after treatment of VTA with vehicle (white bars) or CNO (gray bars). Inactive lever presses are represented with black bars at the bottom. *$P = 0.000075$; two-way ANOVA. (**c**) Effects on horizontal (top graph) and vertical (rearing; bottom graph) locomotion in a familiar environment after inactivating RVP projections to VTA ($n = 11$). Locomotion (beam breaks) during 30 min bins in the 2-h session is shown after VTA microinjection of vehicle (black lines) or CNO (gray lines). (**d**,**e**) Effects on cue-induced and cocaine-primed reinstatement ($n = 9$), as well as horizontal locomotion and rearing ($n = 6$), after inactivation of CVP efferents to VTA. (**f**,**g**) Effects on reinstatement ($n = 11$) or locomotive behavior ($n = 6$) after inactivation of RVP projections to SN. All data are shown as the mean ± s.e.m.

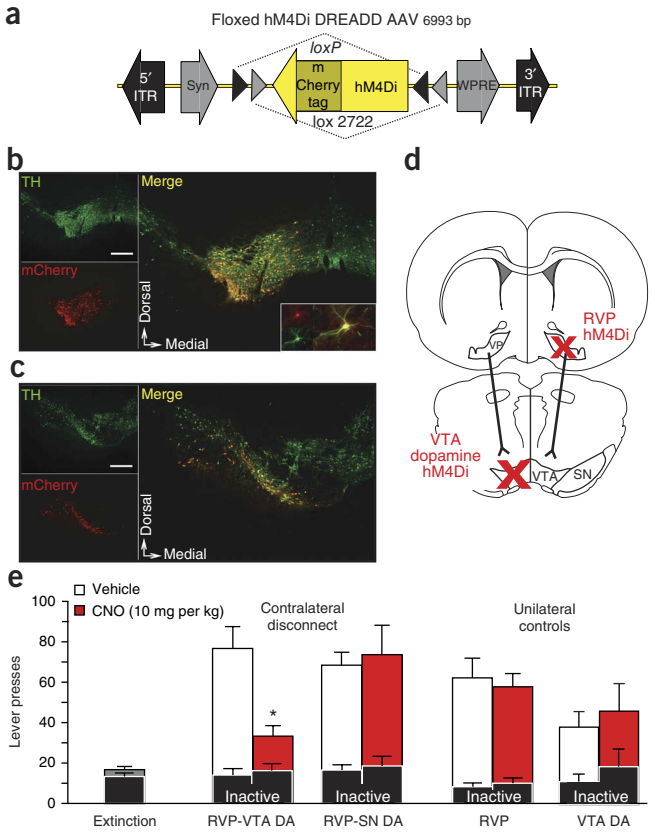

Figure 6 Functional disconnection of rostral ventral pallidum projection to VTA dopamine neurons blocks cue-induced reinstatement. (**a**) A *DIO-Syn-hM4Di-mCherry* AAV construct that was used to selectively express mCherry-tagged hM4Di receptors in dopamine cells in TH::Cre$^+$ transgenic rats. ITR, inverted terminal repeat. (**b**) hM4Di expression in a representative animal with *DIO-Syn-hM4Di-mCherry* injection in VTA. Immunolabeling for TH identifies dopamine neurons (green), and mCherry (red) identifies hM4Di-expressing neurons in VTA. Nearly all hM4Di-expressing neurons were dopaminergic. VTA-injected animals did not show substantial hM4Di expression laterally in SN or in the contralateral VTA. Scale bar, 500 µm. The inset on the right shows a hM4Di$^+$TH$^+$ cell at high magnification (image width, 45 µm). (**c**) hM4Di expression in a representative animal with *DIO-Syn-hM4Di-mCherry* injection in SN. Minimal expression in VTA was observed. Scale bar, 500 µm. Equivalent expression was observed in behaviorally tested rats; VTA, $n = 9$; SN, $n = 8$. (**d**) Unilateral *Syn-hM4Di-HA-GFP* injections were made in RVP, and *DIO-Syn-hM4Di-mCherry* injections were made in the contralateral VTA or SN of TH::Cre$^+$ rats or VTA of Cre$^-$ littermates. When systemic CNO was administered, serial connectivity between the ventral pallidum and midbrain dopamine populations is compromised bilaterally by unilateral hM4Di inhibition of RVP and contralateral hM4Di inhibition of dopamine neurons. (**e**) Active and inactive lever pressing during cue-induced reinstatement in animals with RVP-VTA dopamine (DA) contralateral disconnect. Pressing during late extinction (gray bar at left) and cued reinstatement after vehicle (white bars) or CNO (10 mg per kg body weight; red bars) is shown. Contralateral disconnect animals were TH::Cre$^+$ rats that received unilateral RVP *Syn-hM4Di-HA-GFP* injections and contralateral VTA or SN *DIO-Syn-hM4Di-mCherry* injections. Unilateral RVP inactivation rats (RVP-hM4Di) were Cre$^-$ and received unilateral RVP hM4Di virus plus contralateral VTA dopamine hM4Di virus (although the latter did not cause hM4Di expression in these Cre$^-$ rats). Unilateral VTA dopamine inactivation rats (VTA dopamine hM4Di) were Cre$^+$ and received only unilateral VTA dopamine hM4Di virus. Only contralateral disconnection of RVP from VTA dopamine neurons reduced cued reinstatement below control levels. $^*P = 0.0003$; repeated-measures ANOVA. The group n numbers are listed in the main text. The data are shown as the mean ± s.e.m.

and VTA (not SN) dopamine populations is required for conditioned cues to trigger cocaine seeking during reinstatement.

Further examinations of the nature of the RVP-VTA circuit

GABAergic ventral pallidum projections to VTA can tonically inhibit VTA dopamine neurons[5], and inactivating this projection with DREADDs can disinhibit dopamine neurons (**Fig. 4**). We therefore asked whether disinhibition of VTA dopamine neurons could have contributed to the attenuation of reinstatement we observed after inactivating RVP inputs to VTA with DREADDs. If so, then direct disinhibition of VTA dopamine neurons with the $GABA_A$ antagonist gabazine should also attenuate reinstatement. Instead we observed that intra-VTA gabazine (10 µM, 0.3 µl) strongly increased cued reinstatement ($n = 6$ rats; $F_{2,17} = 9.43$, $P = 0.002$; vehicle as compared

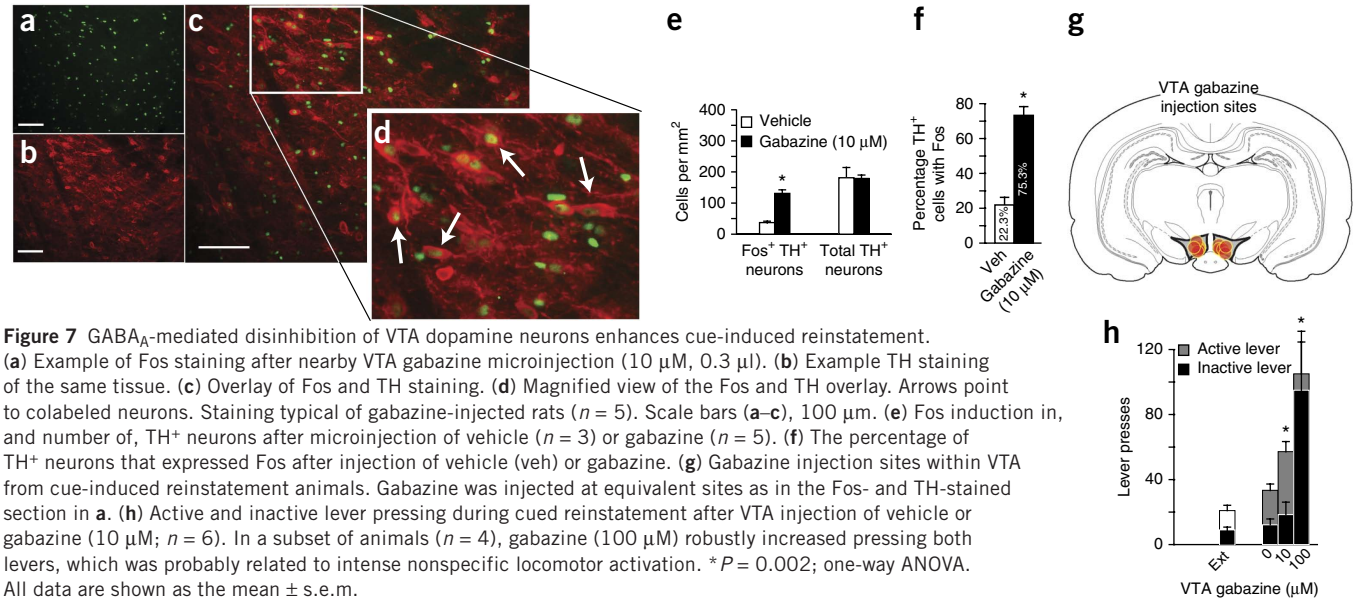

Figure 7 $GABA_A$-mediated disinhibition of VTA dopamine neurons enhances cue-induced reinstatement. (**a**) Example of Fos staining after nearby VTA gabazine microinjection (10 µM, 0.3 µl). (**b**) Example TH staining of the same tissue. (**c**) Overlay of Fos and TH staining. (**d**) Magnified view of the Fos and TH overlay. Arrows point to colabeled neurons. Staining typical of gabazine-injected rats ($n = 5$). Scale bars (**a**–**c**), 100 µm. (**e**) Fos induction in, and number of, TH$^+$ neurons after microinjection of vehicle ($n = 3$) or gabazine ($n = 5$). (**f**) The percentage of TH$^+$ neurons that expressed Fos after injection of vehicle (veh) or gabazine. (**g**) Gabazine injection sites within VTA from cue-induced reinstatement animals. Gabazine was injected at equivalent sites as in the Fos- and TH-stained section in **a**. (**h**) Active and inactive lever pressing during cued reinstatement after VTA injection of vehicle or gabazine (10 µM; $n = 6$). In a subset of animals ($n = 4$), gabazine (100 µM) robustly increased pressing both levers, which was probably related to intense nonspecific locomotor activation. $^*P = 0.002$; one-way ANOVA. All data are shown as the mean ± s.e.m.

to 10 µM gabazine active lever: $t_6 = 2.62$, $P = 0.04$; **Fig. 7g,h**) and robustly induced Fos in nearby dopamine neurons (vehicle, $n = 3$; gabazine, $n = 5$ rats; no effect on number of TH^+ cells: $t_6 = 0.2$, $P = 0.84$; total Fos^+TH^+ cells: $t_{4.4} = 5.55$, $P = 0.001$; percentage Fos^+TH^+ cells: $t_6 = 8.84$, $P = 0.0001$; **Fig. 7a–f**). This finding indicates that simple disinhibition of dopamine neurons is probably not the mechanism by which inhibiting RVP inputs to VTA reduces cued reinstatement.

In addition to GABA projections, RVP sends numerous $VGlut2^+$ efferents to VTA[34]; we asked whether this glutamatergic projection is required for cued reinstatement. We used unilateral DREADD-based RVP inhibition and contralateral VTA microinjection of a cocktail of the AMPA and NMDA antagonists 6-cyano-7-nitroquinoxaline-2,3-dione (CNQX) and D(−)-2-amino-5-phosphonovaleric acid (AP5) (0.7 and 1.6 mM, respectively) to bilaterally compromise glutamate projections from RVP to VTA. This did not affect cued reinstatement ($n = 5$ rats; $t_4 = 1.28$, $P = 0.29$; **Supplementary Fig. 7**). In contrast, reinstatement was attenuated when all VTA neurons were inhibited (with baclofen and muscimol, 0.3 and 0.03 mM, respectively) contralaterally to a DREADD-inactivated RVP (RVP-VTA disconnect, $n = 10$ rats, $t_9 = 2.81$, $P = 0.02$; no effect of unilateral VTA baclofen and muscimol alone, $n = 8$, $t_7 = 1.03$, $P = 0.34$; **Supplementary Fig. 7**). In slices, we also explored whether inhibiting RVP inputs to VTA would decrease spontaneous excitatory transmission (sEPSCs) onto dopamine neurons. CNO (5 µM) had no effect on sEPSC amplitude ($t_5 = 0.22$, $P = 0.83$) or frequency ($t_5 = 0.43$, $P = 0.68$) in TH^+ cells ($n = 6$ cells; **Supplementary Fig. 8**). These findings indicate that RVP glutamatergic projections to VTA do not modulate dopamine neurons directly and are probably not necessary for cued reinstatement.

DISCUSSION

Here we describe an RVP-VTA pathway activated by, and necessary for, conditioned cue-induced reinstatement of cocaine seeking in rats. The involvement of the ventral pallidum in reinstatement depends critically on both the rostrocaudal position within the ventral pallidum and the means by which drug seeking is reinstated (cues or cocaine prime). Cue-triggered drug seeking specifically requires both RVP projections to VTA and functional interactions between RVP inputs and VTA dopamine and nondopamine neurons. In addition to describing a double dissociation between ventral pallidum subregions in drug seeking, we also validate the use of G_i-coupled DREADDs to inactivate specific neuronal pathways through modulation of DREADD-expressing terminals and to functionally disconnect brain circuits *in vivo*.

Ventral pallidum roles in reward seeking

Much previous research has focused on the portion of the ventral pallidum caudal of bregma in rats (CVP), which showed that the ventral pallidum is an important node in mesocorticolimbic reward circuits. Lesions or pharmacological inactivation of CVP reduce drug or food seeking[13,35–38]. Many of these ventral pallidum neurons are spontaneously active, and their GABAergic projection to VTA tonically inhibits populations of dopamine neurons there[5].

Ventral pallidum efferents to VTA are also acutely activated by rewards and associated cues. For example, ventral pallidum–VTA projections in rats are Fos-activated after acute amphetamine administration, cocaine self-administration or cued reinstatement of cocaine seeking[23,39,40], and ventral pallidum neurons phasically fire when salient rewards and their cues are experienced[6,11]. In nonhuman primates, ventral pallidum neurons also fire in relation to reward anticipation, and ventral pallidum inactivation compromises modulation of reward seeking on the basis of reward expectation[22]. Similarly, the ventral pallidum is fMRI-activated by cues for drug or natural rewards in humans[41]. Our report therefore supports and substantially expands on the known roles for the ventral pallidum in reward seeking.

Heterogeneity within the ventral pallidum

Anatomically, both rostrocaudal and mediolateral heterogeneity exists in ventral pallidum cell morphology, transmitter content, sources of afferents and efferent targets[6,10,16,42,43]. A large proportion of the subcommissural RVP consists of a neurotensin-positive ventromedial subregion, which receives afferents from the medial accumbens shell and sends efferents to the mediodorsal thalamus and VTA. In contrast, a large proportion of the sublenticular CVP consists of a calbindin-positive dorsolateral subregion that receives accumbens core inputs and projects to SN and the subthalamic nucleus[1]. RVP (and the adjacent caudal accumbens shell) has been described as a transition zone between the accumbens and traditional (caudal) ventral pallidum, with connectivity and morphological features distinct from those of the rostral accumbens, pallidal or extended amygdala regions[10,42]. Supporting this view, RVP and the caudal ventromedial accumbens shell project similarly to VTA, and Fos activation of both projections is correlated with cue-induced reinstatement behavior (**Fig. 3**)[23].

Previous evidence supports a role for RVP in conditioned motivation and for CVP in the rewarding and priming effects of reinforcers themselves. For example, RVP (but not CVP) is Fos-activated during motivated behaviors triggered by Pavlovian cues for specific salient rewards and is necessary for these cues to trigger seeking behaviors[44,45]. RVP (not CVP) is fMRI-activated when people view highly salient, disgusting photographs, again indicating a role in conditioned motivational states[18]. In contrast, GABA agonists microinjected into CVP reduce cocaine-primed and stress-induced reinstatement of cocaine seeking[35,36], in alignment with our observation that DREADD-based inhibition of CVP neurons blocked primed reinstatement (although to our knowledge ours is the first report of a role for the ventral pallidum, and more specifically, RVP, in cued reinstatement of cocaine seeking). Additionally, CVP (not RVP) has been linked to the hedonic evaluation of primary rewards in animals and humans[18,19].

Here we examined the functions of RVP and CVP in cued and primed reinstatement of cocaine seeking. We showed that RVP (not CVP) is necessary for cues to trigger cocaine seeking, whereas CVP (not RVP) is necessary for a cocaine prime to elicit reinstatement. Therefore, the ventral pallidum in general is critically involved in promoting relapse-related drug seeking, but its rostral and caudal aspects differentially mediate the motivational properties of previously learned cues as compared to cocaine itself.

RVP-VTA projection specifically mediates cued drug seeking

To examine the wider neural circuits with which RVP and CVP interact to drive reinstatement, we focused on ventral pallidum projections to VTA. First we showed that RVP but not CVP projections to VTA are Fos activated in proportion to cued reinstatement. To test whether these RVP efferents to VTA are also necessary for reinstatement, we induced hM4Di DREADD expression in RVP or CVP neurons and then microinjected the DREADD agonist CNO directly into VTA. This allowed us to specifically inhibit ventral pallidum–VTA projections but not other ventral pallidum efferents.

When RVP projections to VTA (but not the adjacent SN) were inactivated in this manner, cue-induced reinstatement was abolished, but primed reinstatement was spared. In contrast, similar inhibition

of CVP projections to VTA failed to affect either cued or primed reinstatement. Therefore, RVP projections to VTA are selectively recruited during cued reinstatement and are necessary for cues to trigger reinstatement, whereas CVP is necessary for a cocaine prime to promote reinstatement through VTA-independent circuitry.

RVP indirectly modulates dopamine neurons in reinstatement

We identified a functional circuit containing RVP and VTA (but not CVP or SN) dopamine neurons that is necessary for cues to elicit reinstatement by functionally disconnecting RVP from VTA dopamine neurons through hM4Di inhibition of RVP in one hemisphere and simultaneous hM4Di inhibition of VTA dopamine neurons in the contralateral hemisphere. This selective, bilateral circuit disruption reduced cue-induced reinstatement, indicating that serial connectivity between RVP and VTA dopamine neurons is required for cues to trigger cocaine seeking.

Ventral pallidum projections to VTA are predominantly GABAergic[3,5,32], and consistent with previous reports[32], we observed that DREADD-based inhibition of RVP inputs to VTA disinhibited dopamine neurons by decreasing sIPSC frequency. However, indiscriminate disinhibition of dopamine neurons is unlikely to account for the attenuated reinstatement that we observed after RVP-VTA inactivation. When we directly disinhibited VTA dopamine neurons (as evidenced by robust Fos induction) with microinjections of the $GABA_A$ antagonist gabazine, cued reinstatement was instead increased (**Fig. 7**). It is therefore likely that reinstatement blockade by inhibition of RVP inputs to VTA involves differential modulation of heterogeneous VTA neuronal subpopulations, possibly including inhibition of nondopaminergic VTA neurons. Notably, this modulation appears to be able to supersede reinstatement-promoting effects of dopamine neuron disinhibition, which can also occur when the RVP-VTA circuit is inactivated. Systematic mapping of RVP inputs to VTA neuronal subpopulations will be required to further characterize the complexities of this new, addiction-related circuit.

In addition to GABA efferents, RVP sends substantial VGlut2-containing projections to VTA[34]. However, DREADD-based inhibition of RVP-VTA projections did not reduce spontaneous excitatory transmission to TH^+ cells, and a contralateral disconnect–based disruption of RVP glutamate projections to VTA did not affect cued reinstatement, arguing against a reinstatement-related glutamatergic RVP-VTA projection.

Conclusions

Here we showed that RVP projections to VTA are activated during, and are necessary for, cue-induced reinstatement and that this requires modulation of VTA dopamine neurons. However, this modulation probably does not involve direct GABAergic or glutamatergic RVP projections onto dopamine neurons. Instead, inhibiting RVP inputs to VTA yielded both excitation of type 1 VTA neurons and inhibition of type 2 neurons *in vivo* (**Fig. 4**). Type 1 neurons, which displayed conventionally dopaminergic electrophysiological characteristics, were excited by ventral pallidum inhibition, consistent with our finding that inactivation of RVP inputs to VTA attenuates GABA inputs to TH^+ neurons (**Fig. 4b–e**). However, indiscriminate disinhibition of dopamine neurons with a $GABA_A$ antagonist did not impede reinstatement but instead robustly facilitated it. Therefore, although our disconnection study revealed that dopamine neurons are needed for ventral pallidum regulation of relapse, the role of the ventral pallidum in reinstatement does not depend on general disinhibition of dopamine neurons in VTA.

One possibility is that ventral pallidum neurons selectively regulate a select subpopulation of VTA dopamine neurons during cued drug seeking. Notably, VTA contains fast-firing, thin-waveform dopamine neurons[46,47], and it is possible that these could be the type 2 neurons whose activity is suppressed after RVP-VTA inactivation (**Fig. 4h,i**). However, this possibility seems unlikely, as inhibitory inputs to dopamine neurons recorded *in vitro* here were nearly always reduced by DREADD-based inactivation of RVP-VTA projections (**Fig. 4e**). Therefore, we hypothesize that complex, subpopulation-specific ventral pallidum modulation of VTA neurons is necessary for cues to elicit relapse to cocaine seeking. These findings call for additional research to characterize the relative connectivity of ventral pallidum GABA, glutamate, acetylcholine and peptide-containing neurons with VTA neuronal subpopulations and to further define the roles for each in reward seeking.

In summary, we have described a new pathway, the projection from RVP to VTA, that is necessary for conditioned drug seeking in a model of relapse in addiction. Furthermore, this circuit-behavior relationship requires RVP modulation of both nondopamine and dopamine VTA neurons. We also showed that ventral pallidum subregions have qualitatively different roles in drug-seeking behavior elicited by either conditioned stimuli or the drug itself. Together these findings both expand the known circuitry of conditioned motivation[48] and also highlight important next directions for untangling the neural substrates of reward-seeking behavior, especially in appetitive disorders such as drug addiction.

METHODS

Methods and any associated references are available in the online version of the paper.

Note: Any Supplementary Information and Source Data files are available in the online version of the paper.

ACKNOWLEDGMENTS

We thank P. Do, M.J. Gilstrap and E.C. Lin for assistance with behavioral testing and immunohistochemistry and B.L. Roth (Department of Pharmacology, University of North Carolina) for DREADD constructs and consultation on DREADDs. CNO was supplied by US National Institutes of Health (NIH) National Cancer Institute (NCI) under the auspices of NS064882-01 and by the National Institute of Mental Health (NIMH) Chemical Synthesis and Drug Supply Program. Research was supported by NIH grants F32 DA026692, K99 DA035251 (S.V.M.), F31 DA030891 (J.T.B.), R21 DA025837 (G.A.-J. and S.P.W.), R01 DA013951 (J.J.W.), R37 DA006214 and P50 DA015369 (G.A.-J.). This project was supported by the National Center for Research Resources and the Office of the Director of the National Institutes of Health through grant number C06 RR015455.

AUTHOR CONTRIBUTIONS

S.V.M. attained funding, designed and conducted experiments, performed surgeries, analyzed data and wrote the manuscript. E.M.V. designed and conducted anesthetized electrophysiology experiments, analyzed these data and wrote the manuscript. J.T.B. designed and conducted slice electrophysiology experiments, analyzed these data and wrote the manuscript. C.R.K. conducted behavioral experiments and wrote the manuscript. E.M.M. performed surgeries for and conducted behavioral and immunohistochemical experiments. J.K. conducted immunohistochemical and confocal microscopy experiments. S.P.W. attained funding and contributed the *Syn-GFP* viral construct. K.D. contributed the TH::Cre transgenic rat line. J.J.W. attained funding, designed and conducted slice electrophysiology experiments and wrote the manuscript. G.A-J. attained funding, designed experiments and wrote the manuscript.

COMPETING FINANCIAL INTERESTS

The authors declare no competing financial interests.

1. Zahm, D.S. & Heimer, L. Two transpallidal pathways originating in the rat nucleus accumbens. *J. Comp. Neurol.* **302**, 437–446 (1990).

2. Zahm, D.S., Williams, E. & Wohltmann, C. Ventral striatopallidothalamic projection: IV. Relative involvements of neurochemically distinct subterritories in the ventral pallidum and adjacent parts of the rostroventral forebrain. *J. Comp. Neurol.* **364**, 340–362 (1996).
3. Kalivas, P.W., Churchill, L. & Klitenick, M.A. GABA and enkephalin projection from the nucleus accumbens and ventral pallidum to the ventral tegmental area. *Neuroscience* **57**, 1047–1060 (1993).
4. Haber, S.N. & Nauta, W.J. Ramifications of the globus pallidus in the rat as indicated by patterns of immunohistochemistry. *Neuroscience* **9**, 245–260 (1983).
5. Floresco, S.B., West, A.R., Ash, B., Moore, H. & Grace, A.A. Afferent modulation of dopamine neuron firing differentially regulates tonic and phasic dopamine transmission. *Nat. Neurosci.* **6**, 968–973 (2003).
6. Smith, K.S., Tindell, A.J., Aldridge, J.W. & Berridge, K.C. Ventral pallidum roles in reward and motivation. *Behav. Brain Res.* **196**, 155–167 (2009).
7. Mogenson, G.J., Brudzynski, S.M., Wu, M., Yang, C.Y. & Yim, C.Y. From motivation to action: a review of dopaminergic regulation of limbic to nucleus accumbens to ventral pallidum to pedunculopontine nucleus circuitries involved in limbic-motor integration. in *Limbic Motor Circuits in Neuropsychiatry* (eds. Kalivas, P.W. & Barnes, C.D.) 193–236 (CRC Press, Boca Raton, Florida, 1993).
8. Churchill, L. & Kalivas, P.W. A topographically organized γ-aminobutyric acid projection from the ventral pallidum to the nucleus accumbens in the rat. *J. Comp. Neurol.* **345**, 579–595 (1994).
9. Heimer, L., Zahm, D.S., Churchill, L., Kalivas, P.W. & Wohltmann, C. Specificity in the projection patterns of accumbal core and shell in the rat. *Neuroscience* **41**, 89–125 (1991).
10. Kupchik, Y.M. & Kalivas, P.W. The rostral subcommissural ventral pallidum is a mix of ventral pallidal neurons and neurons from adjacent areas: an electrophysiological study. *Brain Struct. Funct.* **218**, 1487–1500 (2013).
11. Root, D.H. *et al.* Differential roles of ventral pallidum subregions during cocaine self-administration behaviors. *J. Comp. Neurol.* **521**, 558–588 (2013).
12. Yang, C.R. & Mogenson, G.J. Ventral pallidal neuronal responses to dopamine receptor stimulation in the nucleus accumbens. *Brain Res.* **489**, 237–246 (1989).
13. McBride, W.J., Murphy, J.M. & Ikemoto, S. Localization of brain reinforcement mechanisms: intracranial self-administration and intracranial place-conditioning studies. *Behav. Brain Res.* **101**, 129–152 (1999).
14. Panagis, G., Miliaressis, E., Anagnostakis, Y. & Spyraki, C. Ventral pallidum self-stimulation: a moveable electrode mapping study. *Behav. Brain Res.* **68**, 165–172 (1995).
15. Bengtson, C.P. & Osborne, P.B. Electrophysiological properties of cholinergic and noncholinergic neurons in the ventral pallidal region of the nucleus basalis in rat brain slices. *J. Neurophysiol.* **83**, 2649–2660 (2000).
16. Zahm, D.S. & Heimer, L. Ventral striatopallidal parts of the basal ganglia in the rat: I. Neurochemical compartmentation as reflected by the distributions of neurotensin and substance P immunoreactivity. *J. Comp. Neurol.* **272**, 516–535 (1988).
17. Johnson, P.I., Stellar, J.R. & Paul, A.D. Regional reward differences within the ventral pallidum are revealed by microinjections of a μ opiate receptor agonist. *Neuropharmacology* **32**, 1305–1314 (1993).
18. Calder, A.J. *et al.* Disgust sensitivity predicts the insula and pallidal response to pictures of disgusting foods. *Eur. J. Neurosci.* **25**, 3422–3428 (2007).
19. Smith, K.S. & Berridge, K.C. The ventral pallidum and hedonic reward: neurochemical maps of sucrose "liking" and food intake. *J. Neurosci.* **25**, 8637–8649 (2005).
20. Grace, A.A., Floresco, S.B., Goto, Y. & Lodge, D.J. Regulation of firing of dopaminergic neurons and control of goal-directed behaviors. *Trends Neurosci.* **30**, 220–227 (2007).
21. Tindell, A.J., Berridge, K.C. & Aldridge, J.W. Ventral pallidal representation of pavlovian cues and reward: population and rate codes. *J. Neurosci.* **24**, 1058–1069 (2004).
22. Tachibana, Y. & Hikosaka, O. The primate ventral pallidum encodes expected reward value and regulates motor action. *Neuron* **76**, 826–837 (2012).
23. Mahler, S.V. & Aston-Jones, G.S. Fos activation of selective afferents to ventral tegmental area during cue-induced reinstatement of cocaine seeking in rats. *J. Neurosci.* **32**, 13309–13326 (2012).
24. Armbruster, B.N., Li, X., Pausch, M.H., Herlitze, S. & Roth, B.L. Evolving the lock to fit the key to create a family of G protein–coupled receptors potently activated by an inert ligand. *Proc. Natl. Acad. Sci. USA* **104**, 5163–5168 (2007).
25. Ferguson, S.M. & Neumaier, J.F. Grateful DREADDs: engineered receptors reveal how neural circuits regulate behavior. *Neuropsychopharmacology* **37**, 296–297 (2012).
26. Ungless, M.A. & Grace, A.A. Are you or aren't you? Challenges associated with physiologically identifying dopamine neurons. *Trends Neurosci.* **35**, 422–430 (2012).
27. Ikemoto, S. Dopamine reward circuitry: two projection systems from the ventral midbrain to the nucleus accumbens-olfactory tubercle complex. *Brain Res. Rev.* **56**, 27–78 (2007).
28. Morales, M. & Pickel, V.M. Insights to drug addiction derived from ultrastructural views of the mesocorticolimbic system. *Ann. NY Acad. Sci.* **1248**, 71–88 (2012).
29. Fields, H.L., Hjelmstad, G.O., Margolis, E.B. & Nicola, S.M. Ventral tegmental area neurons in learned appetitive behavior and positive reinforcement. *Annu. Rev. Neurosci.* **30**, 289–316 (2007).
30. van Zessen, R., Phillips, J.L., Budygin, E.A. & Stuber, G.D. Activation of VTA GABA neurons disrupts reward consumption. *Neuron* **73**, 1184–1194 (2012).
31. Stamatakis, A.M. *et al.* A unique population of ventral tegmental area neurons inhibits the lateral habenula to promote reward. *Neuron* **80**, 1039–1053 (2013).
32. Hjelmstad, G.O., Xia, Y., Margolis, E.B. & Fields, H.L. Opioid modulation of ventral pallidal afferents to ventral tegmental area neurons. *J. Neurosci.* **33**, 6454–6459 (2013).
33. Witten, I.B. *et al.* Recombinase-driver rat lines: tools, techniques, and optogenetic application to dopamine-mediated reinforcement. *Neuron* **72**, 721–733 (2011).
34. Geisler, S., Derst, C., Veh, R.W. & Zahm, D.S. Glutamatergic afferents of the ventral tegmental area in the rat. *J. Neurosci.* **27**, 5730–5743 (2007).
35. McFarland, K. & Kalivas, P.W. The circuitry mediating cocaine-induced reinstatement of drug-seeking behavior. *J. Neurosci.* **21**, 8655–8663 (2001).
36. McFarland, K., Davidge, S.B., Lapish, C.C. & Kalivas, P.W. Limbic and motor circuitry underlying footshock-induced reinstatement of cocaine-seeking behavior. *J. Neurosci.* **24**, 1551–1560 (2004).
37. Robledo, P. & Koob, G.F. Two discrete nucleus accumbens projection areas differentially mediate cocaine self-administration in the rat. *Behav. Brain Res.* **55**, 159–166 (1993).
38. Farrar, A.M. *et al.* Forebrain circuitry involved in effort-related choice: injections of the $GABA_A$ agonist muscimol into ventral pallidum alter response allocation in food-seeking behavior. *Neuroscience* **152**, 321–330 (2008).
39. Colussi-Mas, J., Geisler, S., Zimmer, L., Zahm, D.S. & Berod, A. Activation of afferents to the ventral tegmental area in response to acute amphetamine: a double-labelling study. *Eur. J. Neurosci.* **26**, 1011–1025 (2007).
40. Geisler, S. *et al.* Prominent activation of brainstem and pallidal afferents of the ventral tegmental area by cocaine. *Neuropsychopharmacology* **33**, 2688–2700 (2008).
41. Childress, A.R. *et al.* Prelude to passion: limbic activation by "unseen" drug and sexual cues. *PLoS ONE* **3**, e1506 (2008).
42. Zahm, D.S. Is the caudomedial shell of the nucleus accumbens part of the extended amygdala? A consideration of connections. *Crit. Rev. Neurobiol.* **12**, 245–265 (1998).
43. Tripathi, A., Prensa, L. & Mengual, E. Axonal branching patterns of ventral pallidal neurons in the rat. *Brain Struct. Funct.* **218**, 1133–1157 (2013).
44. Leung, B.K. & Balleine, B.W. The ventral striato-pallidal pathway mediates the effect of predictive learning on choice between goal-directed actions. *J. Neurosci.* **33**, 13848–13860 (2013).
45. Robinson, M.J. & Berridge, K.C. Instant transformation of learned repulsion into motivational "wanting.". *Curr. Biol.* **23**, 282–289 (2013).
46. Lammel, S. *et al.* Unique properties of mesoprefrontal neurons within a dual mesocorticolimbic dopamine system. *Neuron* **57**, 760–773 (2008).
47. Luo, A.H., Georges, F.E. & Aston-Jones, G.S. Novel neurons in ventral tegmental area fire selectively during the active phase of the diurnal cycle. *Eur. J. Neurosci.* **27**, 408–422 (2008).
48. Robinson, T.E. & Berridge, K.C. Addiction. *Annu. Rev. Psychol.* **54**, 25–53 (2003).

ONLINE METHODS

Subjects. 159 male Sprague-Dawley rats (250–350 g; Charles River) and 45 outbred male Long-Evans TH::Cre rats (hemizygous Cre^+, $n = 35$; Cre^- littermates, $n = 10$)[33] were single or pair housed in a 12 h, 12 h reverse light cycle vivarium (all tests were conducted in the dark period). No statistical methods were used to predetermine sample sizes, but they were similar to those reported in previous publications[15,19,23,49]. All procedures were approved by the Medical University of South Carolina's Institutional Animal Care and Use Committee.

Surgical procedures. Animals were anesthetized with ketamine, xylazine and meloxicam (56.5, 8.7 and 1.0 mg per kg body weight, respectively) and implanted with indwelling jugular catheters. They then received 20–30 nl injections of 0.5% CTb unilaterally in VTA or 1 µl unilateral or bilateral virus injections into RVP, CVP or VTA. VTA CTb and ventral pallidum lentivirus injections were made by pneumatic pressure using a glass pipette (for CTb, 15–20 µm tip; for lentivirus, 30-45 µm tip) over 5 min and left in place for 15–20 min. In TH::Cre animals, midbrain injections of an AAV floxed *DIO-Syn-hM4Di-mCherry* virus were made over 10 min through a Hamilton microinjection syringe. For bilateral VTA CNO or gabazine or unilateral VTA glutamate antagonist or GABA agonist microinjections in behaving animals, guide cannulae were implanted 2 mm dorsal to VTA or SN.

Viral constructs. To transduce ventral pallidum neurons with hM4Di DREADDs, we used a synapsin promoter–driven lentiviral vector with a GFP reporter custom packaged (VSV-G envelope) by the University of Pennsylvania vector core. To assist with identification, the hM4Di has an N-terminal HA tag and an IRES GFP reporter (*Syn-hM4Di-HA-GFP*; **Fig. 1a**). A *Syn-GFP* lentivirus (lacking the DREADD gene) was used to control for nonspecific virus effects (**Fig. 2b**,**c** and **Supplementary Fig. 5**).

In TH::Cre transgenic rats[33], an AAV containing a double-floxed, inverted open reading frame hM4Di-mCherry sequence (*DIO-Syn-hM4Di-mCherry*; University of North Carolina Vector Core) was microinjected into the ventral midbrain to express hM4Di receptors selectively in TH neurons of VTA or SN (**Fig. 6a**).

Localization of DREADD expression. hM4Di receptor expression in cell bodies and processes was visualized with immunohistochemistry for HA, GFP or mCherry tags (described below). Containment of transduction sites within RVP or CVP, or within VTA or SN dopamine cells, was confirmed by co-staining for substance P (SP; defining borders of the ventral pallidum) or TH (defining VTA and SN) and a brain atlas[50]. A synapsin promoter virus was employed in the ventral pallidum, so some expression was observed outside the borders of RVP or CVP in most animals. Animals with more than 30% of DREADD expression observed outside RVP or CVP were excluded from analyses ($n = 7$). For animals with RVP virus injections, no more than 20% of DREADD-expressing tissue encroached into CVP (i.e., caudal of bregma) or vice versa. Animals injected with the *Syn-GFP* control virus in the ventral pallidum had comparable GFP expression patterns to the hM4Di-injected animals. For TH::Cre rats, hM4Di expression was robust in either VTA or SN and was restricted almost exclusively to TH^+ cell bodies and processes (percentage $mCherry^+$ neurons coexpressing TH (mean ± s.e.m.): 97.5 ± 0.7%; **Fig. 6b**,**c** and **Supplementary Fig. 6**). mCherry expression was not observed in the contralateral hemisphere, and expression did not extend substantially into SN of VTA-injected animals or into VTA of SN-injected animals (**Fig. 6b**,**c**).

Electrophysiological validation of DREADD-based inhibition of ventral pallidum neurons and efferents. Brain slices from animals injected in the ventral pallidum with *Syn-hM4Di-HA-GFP* ($n = 6$ rats) or *Syn-GFP* ($n = 2$) were prepared as previously described[49]. Slice physiology data collection and analyses were not performed blind to the experimental group. Horizontal sections containing VTA were transferred to a 32–34 °C chamber containing a carbogen-bubbled aCSF solution.

Slices were transferred to a recording chamber and perfused with 32 °C aCSF at 2 ml per min. Neurons were visually identified under infrared light using Dodt gradient contrast imaging. Recording pipettes with a resistance of 1–3 MΩ were filled with internal solution containing (in mM) CsCl (120), 4-(2-hydroxyethyl)-1-piperazineethanesulfonic acid (10), $MgCl_2$ (2), ethylene glycol tetraacetic acid (1), Na_2ATP (2), NaGTP (0.3) and 0.2% biocytin; 295 mOsm, pH 7.3. To isolate sIPSCs, recording aCSF was supplemented with AMPA and NMDA antagonists (NBQX and AP5; 10 µM and 100 µM, respectively; Abcam), and for sEPSC recordings, picrotoxin (100 µM; Tocris) was added to the aCSF. Neurons medial to the nucleus of the accessory optic tract were targeted for patch clamp (in the vicinity of dense, GFP-expressing RVP afferents), and whole-cell mode was achieved while holding the cell at −70 mV.

Data were acquired using an Axon MultiClamp 700B amplifier and an ITC-18 digital interface (HEKA Instruments) controlled by AxographX software. Recordings were filtered at 4 kHz and acquired at 10 kHz, and sIPSCs were detected and analyzed using the template-matching event-detection algorithm in AxographX. Detection parameters were set at amplitude >4 pA, and acquired events were visually inspected before averaging. We recorded at least 150 spontaneous currents during a baseline period and after 10 min of 5 µM CNO perfusion. Series resistance (R_s) was monitored throughout the recording, and an experiment was discontinued if the R_s exceeded 25 MΩ or changed more than 25%.

In vivo electrophysiology data collection and analyses were performed in isofluorane-anesthetized rats by an experimenter blind to experimental conditions. Glass recording pipettes (5–12 MΩ) were filled with 2% pontamine sky blue in 0.5 M sodium acetate. A glass injection pipette (20-µm tip) glued ~150 µm behind the recording tip delivered 60 nl of 100 µM CNO to the ventral pallidum or VTA neurons with brief pneumatic pulses. Multiple CNO applications occurred in each animal in different cells, each separated by >30 min. Signals were amplified and filtered (0.3–5 kHz) using a Model 1600 Neuroprobe Amplifier (A-M Systems) and a BMA 200 Bioamplifier (CWE) before digital conversion and recording to Spike 2 (v5.21) with a Micro 1401 MkII interface (CED). Body temperature was maintained at 36.0–37.5 °C throughout the recordings.

Recorded ventral pallidum neurons were located near previous virus injections and were identified by their firing rates and waveforms, as reported previously[12]. For confirmation of recording locations, markings 1 mm above and immediately below recording tracks in each ventral pallidum and VTA site were made by iontophoretic dye deposits immediately before perfusion. VTA type 1 neurons were identified by electrophysiological criteria traditionally describing dopamine neurons[26], including (i) biphasic or triphasic waveform >2.5 ms in duration, (ii) >1.1 ms from spike onset to negative trough and (iii) spontaneous firing rate <10 Hz. All cells included in analyses were from confirmed recordings in the ventral pallidum or VTA.

Drugs and tract tracers. Cocaine HCl (NIDA) was dissolved in 0.9% sterile saline. CTb (Sigma) was dissolved at 0.5% in 0.1 M PBS. CNO was supplied by NIH NCI under the auspices of NS064882-01. For systemic administration, CNO (0, 0.1, 1, 10 or 20 mg per kg body weight) was dissolved in 5% dimethyl sulfoxide and then diluted to a 1 ml per kg body weight volume with 0.9% saline. For intracranial administration, CNO was dissolved in aCSF to 100 µM (*in vivo* electrophysiology) or 1 mM (behavioral microinjection) or 5 µM *in vitro*. Gabazine (10 or 100 µM), baclofen and muscimol (0.3 and 0.03 mM, respectively), and CNQX and AP5 (0.7 and 1.6 mM, respectively; all from Sigma) were dissolved in aCSF for 0.3 µl VTA microinjections.

Behavioral training and testing procedures. Behavioral training and testing took place in standard Med Associates operant chambers described elsewhere[23]. Rats underwent ten daily 2-h self-administration sessions (>10 cocaine infusions per day, 0.2 mg, 50 µl infusion). Pressing one lever yielded a 3.6-s cocaine infusion, tone and light above the active lever (FR1 schedule), followed by a 20-s timeout during which pressing was recorded but did not yield cocaine or cues (**Fig. 2a**). Inactive lever presses were recorded but had no consequences. Animals then received at least 7 d of extinction training (until the criterion of <25 presses for 2 consecutive days was reached) during which lever presses yielded neither cocaine nor cues.

During 2-h cue-induced reinstatement tests, active lever presses yielded cocaine cues but no cocaine. For cocaine priming tests, 10 mg per kg body weight cocaine was administered intraperitoneally (i.p.) immediately before the 2-h test during which lever presses yielded neither cocaine nor cues. For the CTb and Fos experiment, animals were perfused immediately after one of the following 2-h test sessions: CS+ reinstatement, an additional extinction session, exposure to a novel environment or exposure to a discrete CS− (further details are listed in ref. 23).

doi:10.1038/nn.3664

Behavior during the first 30 min of the tests (which most influences Fos protein measured 90 min later) was compared to neuronal activation (**Fig. 3**).

Animals that received systemic CNO had three cued and three cocaine-primed reinstatement tests each. 30 min before each test, animals injected with *Syn-hM4Di-HA-GFP* in RVP (n = 16) or CVP (n = 17), animals injected with *Syn-GFP* in the ventral pallidum (n = 5) and animals with no virus expression (n = 9) received counterbalanced i.p. injections of vehicle and two doses of CNO (0.1 mg per kg body weight: n = 25; 1.0 mg per kg body weight: n = 25; 10 mg per kg body weight: n = 26; 20 mg per kg body weight: n = 30). Other animals received counterbalanced intra-VTA (after RVP or CVP injection of *Syn-hM4Di-HA-GFP*) or intra-SN (after RVP injection of *Syn-hM4Di-HA-GFP*) microinjections of vehicle (aCSF) or CNO (1 mM, 0.3 µl) 5 min before each of two cued and two primed reinstatement tests. Some of these animals were later habituated to an open field for 2 d, and then locomotor activity after vehicle or CNO was tested over 2 d at least 48 h apart (intra-VTA CNO: 0 or 1 mM, 0.3 µl, n = 23). TH∷Cre animals (RVP injection of *Syn-hM4Di-HA-GFP* + VTA injection of *DIO-Syn-hM4Di-mCherry*: Cre^+, n = 9; Cre^-, n = 10; RVP injection of *Syn-hM4Di-HA-GFP* + SN injection of *DIO-Syn-hM4Di-mCherry*: Cre^+, n = 8; VTA injection of *DIO-Syn-hM4Di-mCherry* only, n = 6) received vehicle or CNO i.p. (10 mg per kg body weight) 30 min before each of two cue-induced reinstatement tests. Animals with unilateral RVP injection of *Syn-hM4Di-HA-GFP* + contralateral injection of VTA cannulae underwent three cued reinstatement tests after unilateral VTA injection of vehicle + i.p. CNO (10 mg per kg body weight) and two of the following: intra-VTA baclofen and muscimol + i.p. CNO (n = 12 rats); intra-VTA CNQX and AP5 + i.p. CNO (n = 5); or intra-VTA baclofen and muscimol + i.p. vehicle (n = 8). For bilateral VTA injection of gabazine, animals also underwent two to three reinstatement tests after administration of vehicle and 10 µM (n = 7 rats) or 100 µM (n = 4) gabazine (high-dose testing was discontinued because of intense nonspecific locomotor activation). Vehicle and CNO injection order was counterbalanced in all cases.

Tissue preparation and staining. Animals were deeply anesthetized and perfused with 0.9% saline followed by 4% paraformaldehyde. Brains were postfixed in 4% paraformaldehyde, cryoprotected and sliced at 30–40 µm on a cryostat. For CTb and Fos staining, immunohistochemistry procedures were described previously[23]. To visualize hM4Di expression, we performed immunohistochemistry for HA, mCherry and/or GFP tags. Ventral pallidum borders were defined using immunoreactivity for SP[4], and dopamine cells were identified as TH immunoreactive. All tissue was first incubated in 3% normal donkey serum PBS plus Triton X-100 (PBST; 2 h) and then in primary antibodies in PBST overnight at room temperature. The following primary antibodies were used in these experiments (one or two antibodies per tissue sample): mouse anti-HA (1:500; Covance; MMS-101P), rabbit anti-DsRed (mCherry tag; 1:500; Clontech; 632496), chicken anti-GFP (1:2,000; Abcam; ab13970), rabbit anti-SP (1:5,000; Immunostar; 20064) and mouse anti-TH (1:1,000, Immunostar; 22941). For fluorescent stains, sections were incubated for 4 h at room temperature in fluorescent conjugated secondary antibodies (donkey anti-mouse 488 (HA and TH; 1:500; Invitrogen; A21202), donkey anti-rabbit 594 (DsRed, TH and SP; 1:500; Invitrogen; A21207) and donkey anti-chicken 488 (GFP and Fos: 1:500, Jackson; 703545155)). Slices were mounted and coverslipped with Citifluor mounting medium. For 3,3′-diaminobenzidine visualization of HA, slices were incubated for 2 h in a biotinylated donkey anti-mouse secondary antibody (1:500; Jackson; 715066151) and amplified with an avidin-biotin complex (1:500; Vector). Tissue was dehydrated and coverslipped with Permount. After slice physiology experiments, tissue was fixed for 48 h in 4% paraformaldehyde, sectioned, incubated in 5% normal goat serum PBST (7 min), rabbit anti-TH (1:1,000; Millipore; AB152) and Avidin Texas Red (1:500; Life Technologies; A820) overnight at 4 °C and then incubated in Alexa Fluor 488 goat anti-rabbit IgG (1:500; Life Technologies; A11008) for 2 h. All antibodies were previously validated for specificity, as described on the manufacturer's websites and the *Journal of Comparative Neurology* antibody database.

Quantification of CTb and Fos staining. Fos expression in CTb^+ cells was analyzed as a function of rostral-caudal position within ventral pallidum using a quantification strategy described in a previous report in which other analyses of this tissue were described[23]. Coronal sections at ~250-µm intervals throughout the rostral-caudal extent of the ventral pallidum were photographed at 10× magnification and montaged with the Stereo Investigator Virtual Slice Module (MBF Bioscience) to preserve anatomical landmarks. All CTb^+ neurons (with or without Fos) within the ventral pallidum ipsilateral to the VTA CTb injection were counted on each slice by an observer blind to experimental group, and primary analyses examined the percentage of total CTb neurons that were Fos^+ (**Fig. 3** and **Supplementary Fig. 2**) or the average number of CTb cells per rostro-caudal level (**Supplementary Fig. 3**). To quantify Fos expression in VTA induced by vehicle or 10 µM gabazine, z-stack images were taken at 20× magnification of TH (red) and Fos (green) immunoreactivity 90–110 µm lateral of the VTA microinjection sites (**Fig. 7**). TH^+ and Fos^+ neurons were quantified in Photoshop using ImageJ-deconvolved images. 2–3 images per microinjection were quantified and averaged for each animal.

Analyses and statistics. To examine reinstatement-related Fos expression in VTA-projecting neurons within RVP and CVP, total CTb^+ and CTb^+Fos^+ cells in the ventral pallidum (ipsilateral of VTA CTb injections) were quantified at ~250-µm intervals in each animal. One-way analysis of variance (ANOVA) (with Tukey *post-hoc* comparison) was used to analyze the percentages of Fos^+ CTb neurons between behavioral groups. The average percentages of Fos^+ CTb neurons in RVP (rostral of bregma) or CVP (caudal of bregma) for each animal were also correlated with active lever pressing in the first 30 min of cued reinstatement, 90 min before euthanasia (Pearson's test). For gabazine-induced Fos in VTA, the average numbers of TH^+ and TH^+Fos^+ neurons were computed for each animal after bilateral vehicle (n = 3 rats) or gabazine (n = 5) administration and compared with between-subjects t tests.

The effects of systemic CNO on cued or primed reinstatement were analyzed with mixed ANOVA for CNO dose (between-subjects variable) × lever (active or inactive; within-subjects variable) for each behavioral group (RVP injection of *Syn-hM4Di-HA-GFP*, CVP injection of *Syn-hM4Di-HA-GFP*, *Syn-GFP* injection or no virus). Repeated-measures drug × lever ANOVA tested the effects of CNO in VTA or SN on cued or primed reinstatement in animals injected in RVP or CVP with *Syn-hM4Di-HA-GFP* and systemic CNO on cued reinstatement in TH∷Cre rats. One-way ANOVA was used to test the effects of bilateral VTA-administered gabazine and contralaterally disconnecting RVP from VTA or VTA-administered glutamate on cued reinstatement. Tukey or Bonferroni-corrected t test *post-hoc* analyses were used as appropriate to determine the nature of the significant main effects and interactions. All tests were two tailed, and the normality of the data distribution was tested with Mauchly's test of sphericity (Greenhouse-Geisser corrected if necessary).

For *in vitro* electrophysiology, paired-sample t tests were used to compare the mean spontaneous postsynaptic current amplitudes and frequencies of events during a baseline period and after 10 min of CNO perfusion. Two-way ANOVA with Bonferroni *post-hoc* tests were used to compare the amplitude and inter-event interval cumulative probabilities before and during CNO application. *In vivo*, two-tailed t tests or Wilcoxon signed-rank paired sample tests were used to compare pre-CNO and post-CNO firing rates in the ventral pallidum and VTA (depending on normality computed by D'Agostino-Pearson omnibus test). Silenced neurons were included in the analyses if the original waveform returned within 200 s after CNO application. Baseline firing rates of ventral pallidum neurons were compared using a two-tailed unpaired t test with Welch's correction because of a significant F test for unequal variance.

49. Beckley, J.T., Evins, C.E., Fedarovich, H., Gilstrap, M.J. & Woodward, J.J. Medial prefrontal cortex inversely regulates toluene-induced changes in markers of synaptic plasticity of mesolimbic dopamine neurons. *J. Neurosci.* **33**, 804–813 (2013).
50. Paxinos, G. & Watson, C. *The Rat Brain in Stereotaxic Coordinates* (Academic Press/Elsevier, Amsterdam, Boston, 2006).